SU5: a calibrated variable-polarization synchrotron radiation beam line in the vacuum-ultraviolet range

Laurent Nahon and Christian Alcaraz

SU5 is a high-resolution variable-polarization synchrotron radiation (SR) beam line with which linear and circular dichroism experiments are performed in the vacuum ultraviolet (VUV) range (5–40 eV), based on an electromagnetic crossed undulator called the Onduleur Plan/Helicoïdal du Lure à Induction Electromagnétique (OPHELIE). To get precise knowledge of the polarization state of the emitted SR and to take into account the polarization transformations induced by reflection on the various optics, we set up an *in situ* VUV polarimeter to provide a precise and complete polarization analysis of the SR at the sample location. The overall measured polarization performances were highly satisfactory, with measured linear polarization rates of more than 98% (83%) in the vertical (horizontal) linear polarization mode and an average 92.1% (95.2%) circular polarization rate for the right- (left)-handed circular polarization mode, which, to our knowledge, are the highest reported values in the VUV range. Despite some uneven photon energy efficiency, the OPHELIE crossed undulator behaves as expected in terms of polarization, permitting full control of the emitted polarization by manipulation of the vertical-to-horizontal magnetic field ratio (ρ_{und}) and the relative longitudinal phase (ϕ_{und}).

OCIS codes: 120.2130, 340.6720, 300.6540, 230.6080, 120.5700.

1. Introduction

Polarization, as a geometric characteristic of light, has long been considered an efficient tool with which to probe the geometrical and symmetrical properties of matter by linear dichroism and circular dichroism (CD) experiments that were initially developed for the ultraviolet (UV)–visible range. In the past several decades the use of variable so-called exotic polarizations, namely, rotatable linear and circular, in the vacuum ultraviolet (VUV) and x-ray ranges has allowed one to gather interesting insights into the anisotropic properties of matter. This anisotropy, i.e., handedness, may have a structural, magnetic, electronic, spin, or chiral origin.[1,2] Pioneering circularly polarized synchrotron radiation (SR) beam lines[3] were based on off-plane bending magnet radiation in which flux and circular polarization rates (P_c) had to be compromised. An alternative could be the use of reflection-based polarizers to circularly polarize an initially linearly polarized beam,[4,5] but this would be detrimental to tunability and versatility and introduce additional complexity. On the long-wavelength side of the spectrum, circularly polarized SR in the UV range can be obtained with fast switching of the helicity (several tens of kilohertz) by the use of photoelastic modulators that act as quarter-wave plates, permitting the performance of CD experiments with high sensitivity. Such a method allows one to measure, with lock-in detection, very small relative CD levels, with typical levels near 10^{-4} as in the case of absorption CD of chiral biomolecules. Unfortunately, this technique is limited to the UV range down to ~120 nm because of the cutoff limit of the photoelastic material.[6]

With the rather recent availability of insertion devices based on various magnetic schemes[7–9] that allow one to obtain at the same time both high flux and highly polarized SR, dichroism studies have constituted a rapidly growing field; now a large number of available beam lines on third-generation storage rings are capable of variable polarization. For the sake of completeness, note that VUV–extreme-UV

L. Nahon (laurent.nahon@lure.u-psud.fr) and C. Alcaraz are with the Laboratoire pour l'Utilisation du Rayonnement Electromagnétique, Université Paris-Sud, Bâtiment 209D, B.P. 34, 91898 Orsay Cedex, France. L. Nahon is also with the Commissariat à l'Energie Atomique/Departement de Recherche sur l'Etat Condense les Atomes et les Molecules/Service des Photons, Atomes et Molecules and Laboratoire Francis Perrin/Centre National de la Recherche Scientifique, Unité de Recherche Associée 2453, Bâtiment 522, Centre de Saclay, 91191 Gif sur Yvette Cedex, France.

Received 29 July 2003; revised manuscript received 22 October 2003; accepted 28 October 2003.

0003-6935/04/051024-14$15.00/0

laser-based sources, although they are well suited for time-resolved experiments, do not appear to be competitive with SR as variable-polarization photon sources. Indeed, the availability of circularly polarized laser-based radiation has been limited so far to the low-energy part of the VUV range that is covered by the four-wave mixing technique[10] but is not available at higher energy at which the nonperturbative high-harmonic generation scheme is used, in which the ellipticity of light is obtained to the detriment of flux.[11]

In all SR-based experiments it is often not enough to produce exotic polarized SR. It is also necessary to measure carefully the polarization state of light for several reasons: (i) the insertion device may be imperfect; (ii) electron beam parameter effects such as emittance, energy spread, and close-orbit variations have to be evaluated; (iii) the initial polarization state as emitted by the source may be strongly affected by beam-line geometry and optical surfaces whose effects may, in addition, vary with time because of optical pollution; (iv) the analysis of imperfect polarization (nonpolarized part, residue of the linear component in the case of CD) have to be quantified for a proper scientific data analysis, for instance, for gas-phase CD in the angular distribution of photoelectrons from molecules that are fixed in space.[12] Such precise polarization measurements require the use of dedicated polarimeters that are able to provide a complete analysis of the polarization state of the incoming light, including determination of the nonpolarized part.

If the beam line covers the visible–mid-UV range, the use of an optical setup based on a transmission quarter-wave plate followed by a linear polarizer is possible. Such a technique was used to measure a circular polarization rate (P_c) at a single energy of 75% at 8.4 eV at the Electromagnetic Elliptical Wiggler (ELETTRA) beam line,[13] of 96% at 4.4 eV at the race-track-type storage ring HiSOR,[14] and near unity at ~4 eV at the storage ring NIJI-II.[15] At shorter wavelengths it is necessary to use reflection-based polarimeters such as the one developed at the Photon Factory by Koide *et al.*, who measured $P_c \sim 80\%$ in the 60–80-eV range on the BL11D beam line[16] and 55–90% in the 50–80-eV range on the BL28 beam line.[17] Further into the soft-x-ray range, a polarimeter based on transmission and reflections with multilayer optics[18] was used to commission several beam lines at the Berlin Electron Storage Ring (BESSY) and ELETTRA operating in the water-window range.

In this paper we report on the polarization capabilities of the recently commissioned SU5 VUV high-resolution versatile-polarization beam line,[19–21] which has a double scientific purpose in the 5–40-eV range: (i) providing high resolution for gas-phase spectroscopy with a measured ultimate resolving power of 10^5 to 2×10^5 over the VUV range[21] and (ii) use in exotic polarization studies of anisotropic species, up to 35 eV, such as CD in the valence shell gas-phase photoionization of laser-aligned species,[22] fixed-in-space[23] or chiral[24] molecules, as well as condensed-matter samples. For all these photoionization studies the relative CD level as measured on angular distribution CD by electron spectroscopy is high, typically in the 1–60% range, so moderate helicity switching rates are enough. Besides, part of the second scientific use deals with the biochemical aspect of chirality, especially with the puzzling origin of the homochirality of life. In particular, one is interested in the asymmetric photochemical processes that circularly polarized light may induce on a racemic mixture of amino acids.[25] Here the most important property is the photon flux in a large spectral bandwidth, which has to be maximum to reduce the irradiation duration to ~24 h.

A first analysis with a preliminary optical layout of the SU5 beam line has already been published[26] and has shown the versatility of the available ellipses as produced by its undulator, the Onduleur Plan/Helicoïdal du Lure à Induction Electromagnétique (OPHELIE), including linear and circular polarization modes measured at the sample location, but did not permit a full quantitative analysis of the data because of the limited performances of the VUV (4 + 1)-reflections polarimeter used at that time. Today, with the installation of a new, dedicated *in situ* (3 + 3)-reflections polarimeter, we are able in this paper to report complete polarization calibration and analysis over the whole VUV range for the SU5 beam line in its final layout. To our knowledge this is the first complete report on the polarization analysis of the light emitted by an exotic insertion device in the VUV range.

In Section 2 the undulator OPHELIE is described, followed by a description of the polarization measurement procedure. Then the polarization performance in both the linear and the circular modes is presented and discussed.

2. Electromagnetic Crossed Undulator OPHELIE

The crossed undulator OPHELIE and its commissioning on the Super-ACO storage ring of the Laboratoire pour l'Utilisation du Rayonnement Electromagnétic (LURE; Orsay), including a spectral analysis of the emitted SR, have been described in detail elsewhere.[19,20] Nevertheless, here we recall briefly its principle of operation and main commissioning results to provide the necessary background.

Because of the cumbersome geometry of the SU5 beam line, as depicted in Fig. 1, that includes several reflections on mirrors with incidence angles far from normal or grazing incidence, especially mirror M1,[20] some strong discrepancies in reflectivity and dephasing between the *s* (perpendicular to the plane of incidence) and *p* (in the plane of incidence) components of the incoming SR are induced. Therefore we had to be able to generate any polarization ellipse at the undulator level to obtain pure linear or circular polarization on the sample. For versatility we chose to develop the concept of an Onuki-type crossed undulator,[27,28] the OPHELIE, as a photon source for the SU5 beam line with, in addition and for the first time to our knowl-

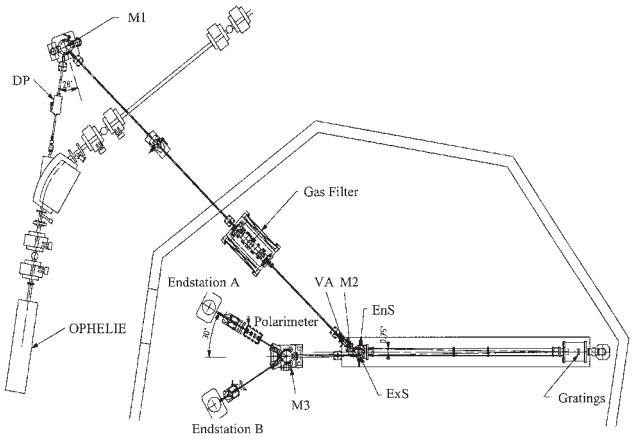

Fig. 1. Schematic of the SU5 beam line located at the center of the Super-ACO storage ring, as viewed from the top: VA, variable-aperture chamber; EnS (ExS), entrance (exit) slit; DP, differential pumping. The whole beam line lies in the horizontal plane, except for arm M1–M2, which is tilted upward by 2°.

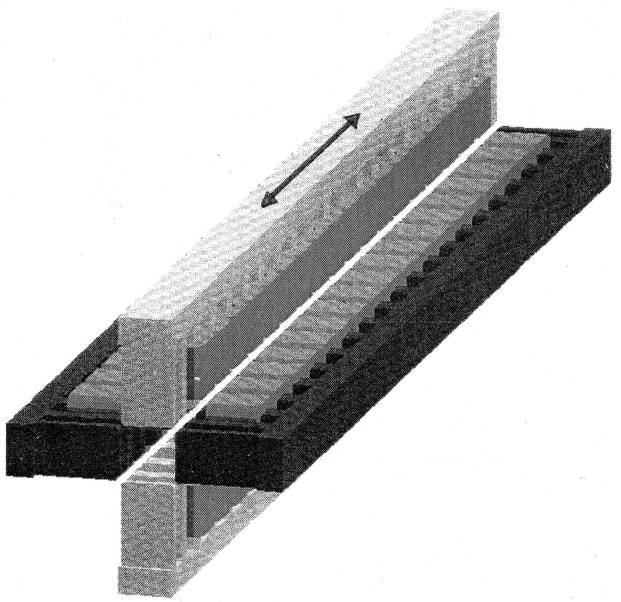

Fig. 2. Schematic of the crossed–overlapped electromagnetic undulator OPHELIE. The only mechanical motion is a longitudinal movement leading to tunable dephasing between −90° and 90°. The gaps are fixed, and the horizontal (B_{0x}) and vertical (B_{0y}) magnetic fields are tunable by varying driving currents I_H (monopolar) and I_H (bipolar) in the main coils.

edge, a fully electromagnetic technology[29,30] that can potentially permit a fast switching speed between left- and right-handed helicity of the photons produced.

The OPHELIE, as displayed in Fig. 2, consists of two identical overlapped and perpendicular planar undulators with nine effective periods of length $\lambda_0 = 25$ cm and a maximum field of 0.126 T (for 200 A driving the main coils), which define, respectively, horizontal and vertical sinusoidal magnetic fields $\mathbf{B}_x$ and $\mathbf{B}_y$. A mechanical translation of the vertical undulator permits relative dephasing (ϕ) between the two undulators, so the on-axis magnetic field is given by

$$\mathbf{B}_t = \hat{u}_x \cdot \mathbf{B}_{0x} \cos\left(\frac{2\pi}{\lambda_0}\mathbf{z}\right) + \hat{u}_y \cdot \mathbf{B}_{0y} \cos\left(\frac{2\pi}{\lambda_0}\mathbf{z} - \phi\right), \tag{1}$$

where z is the longitudinal coordinate and $\hat{u}_y$ ($\hat{u}_x$) is a unit vector in the vertical (horizontal) direction. For a given ϕ, the photon energy of the nth harmonics observed on axis depends not only on the strength of the total peak magnetic field proportional to K_T, where $K_T^2 = K_x^2 + K_y^2$, where $K_{x,y} = 0.934\, B_{0_{x,}\,0_y}\,[T]\,\lambda_0$ [cm], but also on ϕ because of slight magnetic cross talk between the horizontal and vertical magnetic fields via the steel of the poles.[31] Although this effect was not expected, it is not a real problem as long as it is calibrated and taken into account in the computer-control system that drives the OPHELIE. Also, because there is no saturation in the poles, B_{0_x} (B_{0_y}) is a linear function of the main electrical current I_H (I_V) that drives the electromagnets with a proportionality constant of $6.32\ 10^{-4}$ T/A. In practice, the energy calibration that provides the values of the energy of the emitted photons is given by

$$\varepsilon_n[\mathrm{eV}] = n\,\frac{24.32}{1 + 1.089\ 10^{-4}(I_H^2[\mathrm{A}] + I_V^2[\mathrm{A}])[1 + 0.14\ \sin^2(1.1\phi)]}. \tag{2}$$

We have confirmed that indeed the spectrum does not depend on the sign of ϕ or on the polarity of driving current I_V (provided by a bipolar power supply).

The polarization of the light emitted by such a planar–helical undulator depends on the trajectory of the electrons (positrons at the Super-ACO), e.g., as in the following examples: (i) for $\phi = 0$ the total magnetic field is sinusoidal, with a linear pattern in the (xy) transverse plane. For symmetry considerations, the light is linearly polarized in a plane, making an angle α with the horizontal $+x$ axis, where $\tan(\alpha) = -B_x/B_y$. Any value of angle α can be achieved, leading to rotatable linear polarization. For instance, one obtains linear vertical polarization, the standard mode of operation of the beam line in the spectroscopy mode, *a priori* by setting $B_{0y} = 0$. (ii) For $\phi = \pm\pi/2$ and $B_{0x} = B_{0y}$ the total magnetic field is helical, with a circular pattern in the (xy) transverse plane. The light emitted is then circularly polarized, with a helicity that depends on the sign of ϕ (or of B_{0y}). (iii) For neither of these configurations, the polarization is elliptical with any desired required characteristics because, as will be

shown below, there is a one-to-one relation between the three Stokes parameters of the emitted light and the three continuously tunable undulator parameters B_{0x}, B_{0y}, and ϕ. Although the only scientifically interesting polarization at the sample level is purely linear and purely circular polarization, it is important to be able to generate, at any photon energy, any elliptical polarization because a given polarization state will be modified by the various reflections on the optics, which have different complex reflectivities for the *s* and *p* components.

More precisely, the standard Stokes parameters S_1, the linear normal polarization parameter; S_2, the linear 45°-tilted polarization parameter; and S_3, the circular polarization parameter, are defined as

$$S_0 = \langle I_x \rangle + \langle I_y \rangle, \quad S_1 = \langle I_x \rangle - \langle I_y \rangle,$$
$$S_2 = \langle I_{45°} \rangle - \langle I_{135°} \rangle, \quad S_3 = \langle I_+ \rangle - \langle I_- \rangle, \tag{3}$$

where S_0 stands for the total flux and where $\langle I_u \rangle$ are the mean intensities measured on the u axis. This includes the particular case of $\langle I_\pm \rangle$, the right–left circular polarization intensities, for which $u\pm = \pm(1/\sqrt{2})(u_x \pm iu_y)$ if we choose the following conventions for the electrical fields associated with polarized light:

$$E_{x,y} = E_{0x,y} \exp[i(\omega t - kz + \delta_{x,y})].$$

As a function of the amplitudes of these fields one gets

$$S_0 = [(E_{0x})^2 + (E_{0y})^2],$$
$$S_1 = [(E_{0x})^2 - (E_{0y})^2],$$
$$S_2 = 2E_{0x}E_{0y} \cos(\delta_x - \delta_y),$$
$$S_3 = -2E_{0x}E_{0y} \sin(\delta_x - \delta_y), \tag{4}$$

where we have chosen the following handedness convention: pure right-handed circular polarization (i.e., $\langle I_+ \rangle / I_0 = 1$ and $S_3/S_0 = 1$) corresponds to $\delta_x - \delta_y = -90°$ and corresponds, for a fixed z, to the rotation of the field with time clockwise for an observer looking the light coming to him (see Ref. 32 for a discussion of conventions).

In theory, at the exit of the undulator OPHELIE the three partial polarization rates P_i (i = 1–3), defined by $P_i = S_i/S_0$, are linked to the three parameters K_x, K_y, and ϕ by means of[19,33]

$$P_1 = \frac{S_1}{S_0} = \frac{K_y^2 - K_x^2}{K_x^2 + K_y^2} = \frac{\rho^2 - 1}{1 + \rho^2}, \tag{5}$$

$$P_2 = \frac{S_2}{S_0} = -\frac{2K_xK_y \cos(\phi)}{K_x^2 + K_y^2} = -\frac{2\rho \cos(\phi)}{1 + \rho^2}, \tag{6}$$

$$P_3 = \frac{S_3}{S_0} = -\frac{2K_xK_y \sin(\phi)}{K_x^2 + K_y^2} = -\frac{2\rho \sin(\phi)}{1 + \rho^2} = P_c, \tag{7}$$

where ρ is the magnetic strength ratio, given by $\rho = K_y/K_x$. From Eqs. (5)–(7) it is clear that, by setting the proper parameters, one can produce any polarization state of the light at any photon energy, as we shall see in Section 4 below. Besides, one can measure CD simply by switching the polarity of the current driving the vertical magnetic field, i.e., by switching the sign of ρ.

Until now we have considered only the ideal case of a filament beam passing through a perfect undulator and observed at infinity on axis, such that the emitted SR is fully polarized. Of course, in reality there are several causes of depolarization, such as nonzero emittance and beam-energy spread effects, the angular integration by the beam line, and possible misalignment, imperfect monochromatization, and magnetic defects and inhomogeneities (mostly transverse fields gradients) of the OPHELIE. All these effects lead to a total polarization rate smaller than unity because part of the light is nonpolarized, so one can write

$$S_0 = (S_1^2 + S_2^2 + S_3^2)^{1/2} + S_4, \tag{8}$$

where S_4 is the intensity of the unpolarized part of the emitted light.

A dc on-beam commissioning of the OPHELIE was performed[31] both in terms of the emitted spectrum and in terms of electron beam parameters, allowing one to determine the value of the currents to be set in the compensation and correcting coils located at the entrance and the exit of the undulator as a function of main coils currents I_H and I_V such that, for any value of ϕ, the close orbit stays within 0.3 mm of the nominal orbit. Then a position feedback system acting on correction coils located around the whole storage ring locks the positron trajectory onto the nominal orbit.[34] Finally, coupling and tuning variations are minimized owing to the use of a dedicated feedback system, leading to possible ac switching operation of the OPHELIE controlled from the SU5 end station computer, from I_V to $-I_V$ within ~30 s, in a manner that is transparent to other users of the ring. Of course, such speed does not permit the determination of very small CD signals ($\ll$1%), which are anyway beyond the scientific scope of SU5 and which would require the lock-in detection associated with fast modulation and switching techniques in the kilohertz range.

3. Beam-Line Optical Layout and the Polarization Measurement Procedure

The geometry and the setting of the different optical elements of a beam line as depicted in Fig. 1 for SU5 can have a strong influence on the polarization of the SR light impinging upon the sample. Indeed, the polarization modifications induced by the reflection of incoming light by an optical reflecting element can be described by a 4 × 4 Müller matrix[35] acting on the $\mathbf{S}(S_0, S_1, S_2, S_3)$ incoming light's quadrivector. The Müller matrix elements depend on Ψ, where $\tan \Psi = |r_p/r_s|$ is the modulus of the ratio of the complex reflectivities, given by

$$r_{p,s} = |r_{p,s}| \exp(i\delta_{p,s}), \tag{9}$$

and on the induced relative phase shift $\Delta = \delta_p - \delta_s$. One can then estimate the effect of the whole beam line on the polarization state by multiplying the Müller matrices of each mirror involving the n and k Fresnel energy-dependent constants as given in the literature,[36] including the necessary rotation matrices to transform the (x, y) coordinates of the laboratory frame into the (p, s) coordinates of each mirror. Of course, when the optics are positioned at a grazing-incidence angle, such as on soft-x-ray beam lines, the Müller matrices reduce to nearly unity, so there is almost no transformation of the initial polarization state by the beam line. However, considering the different incidence angles as shown in Fig. 1, this restriction does not apply to SU5, so we have to invert the overall matrix, i.e., to determine experimentally the Stokes parameter of the SR to be emitted by the undulator OPHELIE and thus the undulator's main parameters (K_x, K_y, and ϕ) as given by Eqs. (5)–(7). This inversion leads, after transformation by the whole SU5 beam line, to the desired (linear or circular) polarization state at the sample location. Such an SU5 matrix (M_{SU5}) inversion can be expressed as

$$\mathbf{S}_{\mathrm{und}}(K_x, K_y, \phi) = M_{\mathrm{SU5}}{}^{-1}(\omega)\mathbf{S}_{\mathrm{sample}}, \qquad (10)$$

and its experimental practical determination is presented in Section 4 below.

A. Beam Line's Optical Layout

The beam-line's optical layout has been described in detail elsewhere.[20] Briefly, the SR emitted by the undulator is deflected and refocused onto the center of a harmonic suppressor gas filter[37] by toroidal mirror M1 (Fig. 1) operating with a 28° incidence angle in the horizontal plane, thus inducing a strong difference (modulus and phases) between the s and p components of light. In addition, M1 also deflects the beam by a 2° angle in the vertical plane to permit the SR to avoid the ring vacuum vessel. Such dual horizontal–vertical deflection couples the horizontal and vertical polarization, which does not correspond anymore to the pure p and s components of light as they refer to the M1 orientation. We shall see below that this result has some moderate but real influence on the polarization. Note that mirror M1 is in fact a dual component with two optical surfaces that are moved in vacuum in front of the impinging SR for optimum reflectivity over the whole VUV range, with mirror M1(A) made from bare solid SiC for the 5–20-eV range and mirror M1(B) made from Pt-coated SiC for the 20–40-eV range. Then the SR emerging from the center of the gas filter enters a variable-aperture chamber, in which are located four blades mounted onto micrometer-resolution translation stages that allow precise tuning of the (square-shaped) solid angle to be collected by the beam line. This is an important issue because it is well known that the polarization state and the total polarization rate of the SR emitted by an undulator strongly depend on the beam-line collection angle with respect to the diffraction-limited central cone emission of light, which scales as $(\lambda/2L)^{1/2}$ (rms), where λ is the wavelength of interest and L is the total length of the undulator (2.5 m here).[38]

Downstream from the four-blade aperture chamber the SR is deflected by toroidal mirror M2 (bare Si, 75° incidence angle) and refocused onto the entrance slit of a 6.65-m Eagle off-plane monochromator. The monochromator is equipped with two gratings (0.75° incidence angle): a 2400-groove/mm bare SiC grating (G1) for the 5–21-eV range and a 4300-groove/mm Pt-coated grating (G2) for the 15–40 eV range, which allow one to reach ultimate resolving powers in the 100,000–200,000 range.[21] Note that in the off-plane configuration the deflection angle that is due to the gratings is in the horizontal plane, whereas the diffraction plane is vertical, with a vertical scanning angle that varies from 0 to 17°, depending on the wavelength and on the choice of grating. Nevertheless, in terms of its effects on polarization, the deflection is purely in the horizontal plane, so the gratings do not couple horizontal and vertical polarization as mirror M1 does. In addition, calculations beyond the scalar approximation that take into account the explicit shape of the grating's horizontal grooves do not show a significant depolarization effect, or a modification of the polarization, as a result of diffraction by the gratings.[39] Such an assumption is confirmed by the fact that the linear and circular polarization rates, as described below, do not exhibit a specific trend in magnitude with the photon energy, i.e., with the diffraction angle of the gratings. A similar argument can also be used to justify neglect of the effects of light scattering on the various optics.

After the exit slit, the monochromatized SR is deflected and refocused toward one of the two end stations, A or B, by toroidal postfocusing mirror M3 (bare Si, 75° incidence angle; Fig. 1). After the last optics, on end station A branch of mirror M_3 is installed a dedicated polarimeter that therefore permits the measurement of the polarization state of the light immediately before the light impinges onto the sample located downstream. Note that the measured polarization state is exactly the same as that of the light that would strike a sample located at end station B after a switch (rotation by 210°) of mirror M3, so in practice the polarization calibration is valid for both beam-line branches.

B. Polarimeter

The methods of polarization measurement are similar to those of the classic polarimetry textbook experiment in the optical range, in which a quarter-wave plate induces a 90° phase shift between the s and p components of the incoming light and an analyzer plate ideally transmits only the s component. Then independent rotation of both optical elements about the photon beam's axis permits precise measurement of the polarization state of the incoming light. But we note that polarimetry measurements made with only one rotating optical element[40] are not able to

disentangle circular polarization rate P_c from the unpolarized part of light, S_4/S_0.

More precisely, in the general case of a polarimeter composed of a first dephasing optical element (element 1) with azimuthal angle α and overall complex reflectivity characterized by (Ψ_1, Δ_1) and of a second analyzing element with azimuthal angle β and overall complex reflectivity characterized by (Ψ_2, Δ_2), the transmitted light's Stokes vector (S_f) can be written as[16,18,41]

$$\mathbf{S}_f = R(-\beta)M_2(\Psi_2, \Delta_2) \times R(\beta)R(-\alpha)M_1(\Psi_1, \Delta_1)R(\alpha)\mathbf{S}_i, \qquad (11)$$

where R(α) and R(β) are the rotation matrices that correspond to the transformation of coordinates induced by the azimuthal rotation or angles α and β, respectively. M_1 and M_2 are, respectively, the Müller matrices of the first and second optical elements, and $\mathbf{S}_i$ is the Stokes vector of the light incoming toward the polarimeter. The transmitted intensity, as measured by a detector located downstream of the polarimeter and on the rotation axis, is given by the first component of (S_f) as

$$(\mathbf{S}_f)_0 = Cf(S_1/S_0, S_2/S_0, S_3/S_0, \Psi_1, \Psi_2, \Delta_1; \alpha, \beta), \qquad (12)$$

where C is a normalization factor and the function f is given by Eq. (8) of Ref. 16. f is a nonlinear function of two variables (α and β) and of seven unknown parameters (C, S_1/S_0, S_2/S_0, S_3/S_0, Ψ_1, Ψ_2, and Δ_1). By measuring the transmitted flux for several (more than seven) configurations (α, β), one can deduce through a fitting procedure with Eq. (12), the three reduced Stokes parameters (S_1/S_0, S_2/S_0, S_3/S_0) that one is interested in, without making any assumptions about the polarimeter-related optical constants (Ψ_1, Ψ_2, and Δ_1) because they are also derived for each data set by the fitting procedure.

A detailed description of the general optomechanical conception, commissioning, and performance analysis of the polarimeter will be the subject of a forthcoming paper.[41] Briefly, the practical requirement for our polarimeter is that it should permit at any moment, in vacuum, the precise measurement of the complete set of Stokes parameters, including S_4/S_0 as given by Eq. (8) from the parameters fitted from Eq. (12), allowing us if necessary to change the OPHELIE's parameters to obtain the desired polarization state at the polarimeter level, i.e., at the sample level.

As no transmitting materials are transparent over the whole VUV range, we decided to use reflecting elements. The concept is close to the one proposed by Koide *et al.*,[42] who used triple reflections on two faces of a prism and on one plane mirror for each of the two optical elements, as shown in Fig. 3. For the optimal compromise between dephasing (Ψ_1 close to 45° and Δ_1 close to 90°) and analyzing (Ψ_2 close to 0°) properties and reflectivities over the whole VUV range we chose to install three Au-coated prisms for the dephasing element with 140°, 150°, and 160° opening angles and two Au-coated prisms for the analyzing element with 130° and 140° opening angles.[41] All these prisms are interchangeable in vacuum and can be removed by linear translation motion from the SR beam path to allow the beam to go directly toward the sample. The mechanisms for azimuthal rotation, which are actuated through ball-bearing systems, have been especially designed with care to achieve a high coaxial coincidence of the two rotation axes. Note that such high mechanical precision was not achieved with the previous nondedicated polarimeter that we used for the preliminary polarization measurement campaign,[26] and that prevented us from getting accurate quantitative results.

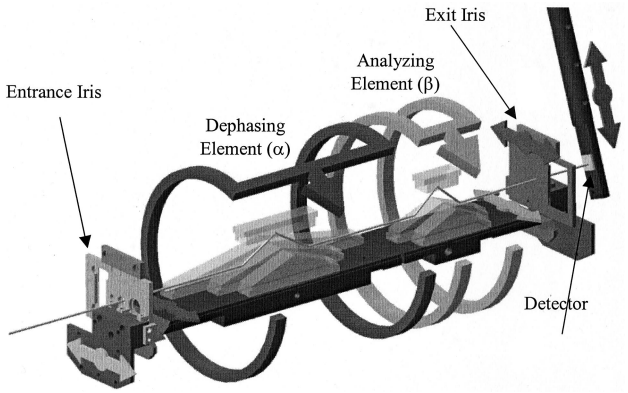

Fig. 3. Schematic of the SU5 (3 + 3)-reflection polarimeter, showing the dephasing and analyzing elements to be rotated by respective angles α and β, which involve, respectively, three (140°, 150°, and 160°) and two (130° and 140°) prisms. One can also see the two irises and the movable UV–XUV detector. The prisms can be moved out of the way of the photon beam to allow the beam to move toward the sample.

C. Polarization Measurement Procedure

Before the polarization measurement is made, one spatially filters the SR beam by setting the variable aperture such that the acceptance angle of the SR coincides with the diffraction-limited central cone aperture of the undulator, ranging from 475 μrad at 6 eV to 220 μrad at 28 eV (Subsection 3.A). An off-axis collection angle that is too large would give rise to a red-side tail of the peaks and to an enhancement of the even-order harmonics whose polarization is not well defined. Then mirror M1 is aimed such as to maximize the flux through the gas filter apertures while the monochromator is set to the blue side of the undulator peak (fundamental or odd harmonics) to ensure that the beam-line collection axis coincides with the undulator's magnetic axis. Note that the 6.65-m monochromator is operated, for polarization measurements, with a typical slit width of 500 μm. With a dispersion of 0.06 (0.033) nm/mm in the exit slit plane for grating G1 (G2), a 500-μm slit aperture corresponds to typically 1 meV near 6 eV (for G1) and 10.5 meV near 28 eV (for G2). This quite high spectral purity ensures that nonmonochromatic effects on the measured polarization can be neglected.

The polarimeter is then carefully aligned with respect to the SR axis, with the prisms out of the beam. One achieves this alignment by inserting in vacuum a 2-mm-diameter entrance iris (Fig. 3) on the mechanical axis of the polarimeter and then maximizing the signal from a dedicated in-vacuum movable XUV photodiode by manipulating the horizontal and vertical translation system operating at the polarimeter entrance level. A similar setting is made with the horizontal and vertical translation system operating at the polarimeter exit level by insertion of an additional 1.6-mm-diameter iris at the exit level. Once the polarimeter is aligned, the two irises are removed, and a simple large rectangular aperture is installed at the entrance location to limit stray light.

The prisms of elements 1 and 2 are then chosen, and inserted, according to the energy of the photons whose polarization ellipse is to be determined. The polarization measurement can then start. It consists of measuring the flux transmitted through the polarimeter, typically for 15 α angles and 20 β angles, i.e., for 300 points, which takes typically 30–90 min, depending on the accumulation time at each point. Frequently a reference normalization signal that corresponds to a given (α, β) configuration is recorded to take into account the decrease in SR flux over the measurement time. Also, the background signal, recorded with the SR shutter off, is frequently precisely determined to allow a possible drift in the detector's dark-count signal to be taken into account. After application of the normalization procedure and subtraction of the background, the (α, β) spectrum is fitted with Eq. (12), providing the seven parameters (C, S_1/S_0, S_2/S_0, S_3/S_0, Ψ_1, Ψ_2, and Δ_1) for a given photon energy and a given (I_H, I_V, ϕ) OPHELIE configuration.

The quality of the fitted curve and therefore the errors bars on the Stokes parameters strongly depend on the optomechanical precision of the polarimeter as well as on the signal-to-noise ratio of the acquired data, as is discussed in detail in Ref. 41. Typically, error bars on the measured Stokes parameters are ~1% for the linear mode and ~2% in the circular mode. In the latter case, when the linear polarization rate of the light to be measured is really close to zero, it will be mathematically impossible for the fitting procedure to extract S_3/S_0 without knowledge of other unknown polarimeter parameters (Ψ_1, Ψ_2, and Δ_1).[41] Hence the measurement of such polarization is made in two steps. A first polarization measurement is made at strictly the same photon energy but at a different setting of the undulator for which nonzero linear polarization is produced at the sample location. This permits the determination of the polarimeter parameter at this photon energy. The second step is the measurement of the quasi-circular polarization by fitting the data set by use of the same and fixed polarimeter parameters, because they depend only on the photon energy.

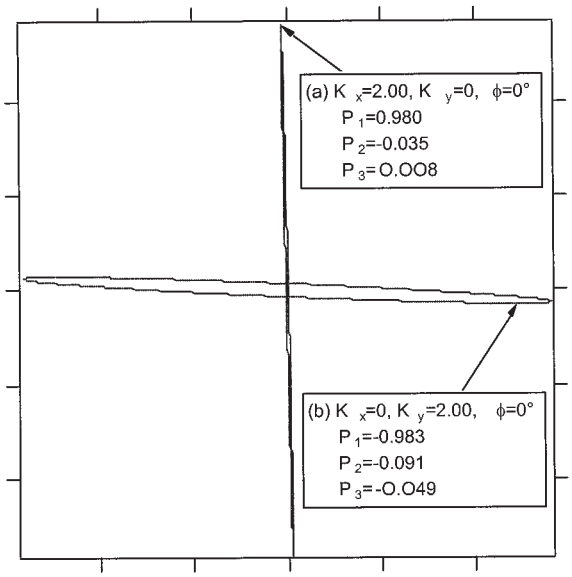

Fig. 4. Polarization ellipses at the sample location recorded on the maximum of the undulator's fundamental peak at 8.85 eV for pure linear polarization emitted by the undulator: (a) I_H = 135 A (K = 2.00), I_V = 0 A, and ϕ = 0°, leading to a vertically polarized emitted SR; (b) I_H = 0 A, I_V = 135 A (K = 2.00), and ϕ = 0°, leading to horizontally polarized emitted SR.

4. Polarization Measurements and Discussion

We now present the measured polarization properties of the whole SU5 beam line, including its source, the undulator OPHELIE, underlining the roles of both the optical beam line and the undulator. For the latter, the properties are especially interesting because the two Onuki-type undulators in operation have been characterized so far only on the fundamental peak by direct optical methods in transmission in the visible[43] and the near-UV,[15] whereas here we extend the analysis toward the VUV range for both the fundamental and the harmonics (third and fifth).

A. Linear Polarization

A priori, the production of linearly polarized SR is straightforward: The use of only the horizontal (vertical) undulator, i.e., with I_V = 0 (I_H = 0), should provide vertical (horizontal) polarized radiation. In practice, one has to be careful with the effects of the optical beam line, especially in our case with respect to the dual horizontal and vertical deflection achieved by the first mirror, M1, as we shall see below.

In Fig. 4 we present the ellipses that correspond to both elliptical and circular polarization recorded at 8.85 eV with (a) I_H = 135 A (K = 2.00), I_V = 0 A, and ϕ = 0°, leading to a vertically polarized emitted SR, and (b) I_H = 0 A, I_V = 135 A (K = 2.00), and ϕ = 0°, leading to a horizontally polarized emitted SR. Although the linear character of both polarizations is well maintained, with P_1 values of ±0.98 one can clearly see the differences in the distortions induced by the beam line for the two cases. The vertically polarized SR is affected by only a slight rotation that is due to the 2° vertical elevation angle of the beam

line on arm M1–M2 (Fig. 1), leading to a nonzero value for P_2 (-0.03%), but the ellipse is very flat ($P_3 < 0.01\%$). This rotation can be seen as due to the rotation matrix transforming the (x, y) laboratory frame coordinates into the M1 (s, p) coordinates, which has a nonzero coupling element between S_1 and S_2. For horizontal case polarization, not only do we observe the rotation, which is slightly more important in absolute value ($P_2 = 0.09$), but in addition there is a circular component ($P_3 = -0.05$), leading to a nonzero ellipticity. As mentioned above, this effect is due to the s–p coupling achieved by mirror M1 because of its dual orientation. Here the linear horizontal polarization corresponds mostly to p polarization but also has a nonzero s component. The s–p mixing induces a vertical linear component that, compared to the horizontal component, is comparatively amplified by the whole beam line. Such is not the case when one starts with vertical linear polarization, for which the M1-induced horizontal component is comparatively diminished.

We have observed this trend at several photon energies, with more-pronounced ellipticity observed at low photon energies (as little as 5.9 eV), where the transmission of the horizontally polarized radiation is especially weak compared with that of the vertically polarized radiation, leading to a maximum measured P_3 value of 0.17, at 5.9 eV, in good agreement with the value of 0.18 deduced from published optical constants.[36] We have not tried to compensate for this effect by manipulating the undulator parameters to induce S_2 and S_3 components at the undulator level because in most of the covered energy range this effect is limited, especially if one considers that for most experiments it is the squared values of the Stokes parameters that are to be taken into account.

As a consequence, the standard linear polarization of the beam line is vertical because it is purer in terms of polarization and it provides more flux, typically 2–5 times more than in the horizontal polarization mode because higher reflectivities depend on the photon energy. For this standard mode of operation, which is frequently used for spectroscopy, we have carefully checked the polarization state over the whole fundamental peak of the undulator with fixed settings, which can be an issue when one performs large spectral scans of 1 eV or more. An example of a peak centered near 10.3 eV is shown in Fig. 5 for three polarization measurements: one on the top, one on the blue side, and one on the red side of the peak. In all three cases the result is highly satisfactory, with a vertical linear polarization rate P_1 greater than 98% over the whole fundamental peak and nearly 100% on top. The total polarization rate ($P_{\text{tot}} = 1 - S_4/S_0$) is a bit smaller (98.4%) on the red side of the peak, which is not surprising because the red tail corresponds to a large extent to the off-axis contribution of the undulator emission, which in the linear case gives rise to an increased S_4 nonpolarized contribution (by as much as 1.6% near 9.5 eV).

We performed measurements of linear polarization rates throughout the whole VUV range by changing the undulator parameters according to Eq. (2) and setting the monochromator at different peak energies of the undulator spectrum. The results are summarized in Fig. 6. For vertical linear polarization the measurements are highly satisfactory, with the value of P_1 in the range -0.98 to -1.00. These values are in good agreement with numerical calculations that take into account the geometry of the whole beam line and the published optical constants, which indicate values of -0.993 to -0.997 over the whole VUV range. Here one probably reaches the limit of the error bars in the measurements and the limit in the SR polarization because of the finite emittance and collection angle. Note that we analyzed the polarization for numerous energies in the vertical linear mode partly because, as we explained above, the polarization analysis for circular polarization requires previous measurement with noncircular polarization to extract the optical constants of the polarimeter that cannot be derived directly in the purely circular

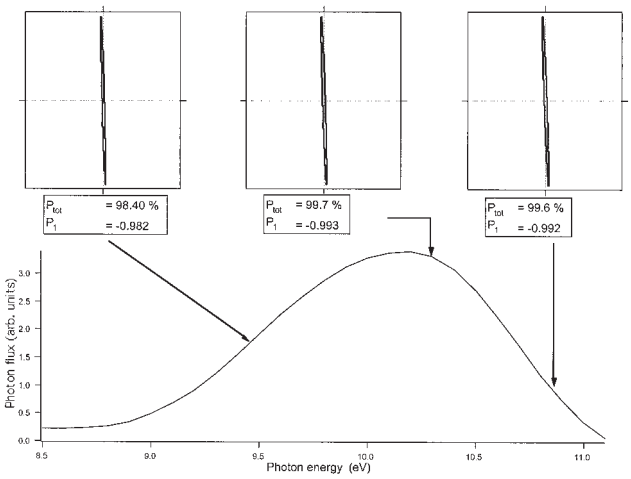

Fig. 5. Undulator spectrum corresponding to $I_H = 117$ A ($K = 1.72$), $I_V = 0$ A, and $\phi = 0°$, leading to a vertically polarized emitted SR, together with polarization ellipses measured at three photon energies. $P_{\text{tot}} = 1 - S_4/S_0$ corresponds to the total polarization rate.

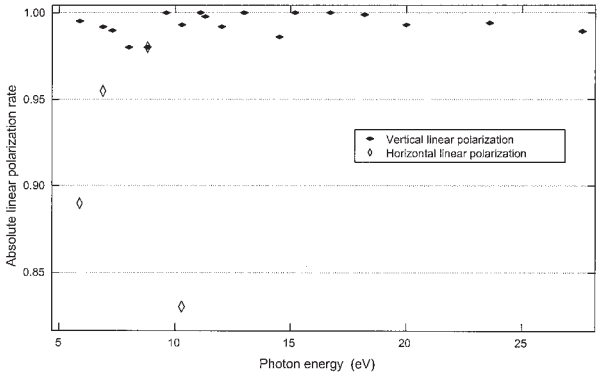

Fig. 6. Absolute normal linear polarization rates, modulus (S_1/S_0), as measured in vertical (H undulator alone) and horizontal (V undulator alone) linear modes for several photon energies. The relative errors bars are typically 1%.

case.[41] The horizontal linear mode is much less used, and for that mode we analyzed the polarization at only a few photon energies. The linear polarization rate in the horizontal mode is satisfactory but in general is not as not so good as in the vertical linear mode. This result is due to the nonnegligible ellipticity (nonzero S_3) but also to the increased emission of unpolarized light, by as much as 16% at 10.3 eV, for the horizontal polarization. This effect is probably due to the imperfect magnetic fields produced by the vertical undulator, which produce a skewed trajectory, leading to some off-axis influence on the observed emission, which explains why the P_1 values are in general below the calculated values of ~0.98 over the whole VUV range. This effect becomes stronger, and can be seen in the less intense and broader undulator spectrum, as one decreases the K value of the vertical undulator, for instance, between 10.5 and 15 eV where one uses a small K value on the fundamental (after 15 eV, one uses high K values on the third harmonics). No specific attempts were made to measure precisely the polarization rates above 10.5 eV for horizontal polarization, but measurements of the angular distribution of photoelectrons produced by the photoionization of Ar at 16–25 eV suggest a polarization rate above 90%.

Linear dichroism experiments are performed by driving alternately one undulator and then the other, switching the polarization state from $S_1 \sim +1$ to $S_1 \sim -1$. Note also that we could obtain 45° tilted linear polarization by switching on both undulators with the same current and a zero phase if we neglected the effect of the beam line, leading to the performance of linear dichroism experiments by switching the polarity of I_V such that the polarization state would alternate from $S_2 \sim +1$ to $S_2 \sim -1$. Here the effect of the beam line is so strong that at the sample location the polarization does not correspond at all to linear polarization. No specific attempts were made to find the correct ellipse to start with at the undulator level, which would correspond to a pure 45° tilted linear polarization at the sample location.

B. Circular Polarization

The calibration of circular polarization is much more difficult than that of linear polarization. Indeed, because the cumbersome geometry of the beam line strongly affects the polarization state from the undulator to the sample, the calibration departs strongly from the trivial configuration: $I_H = I_V$ and $\phi = \pm 90°$. Therefore the calibration problem consists in solving Eq. (10), i.e., in finding for each photon energy the correct polarization ellipses at the undulator level. These ellipses will be transformed, through the beamline, into pure left- and right-handed circular polarization at the sample level, i.e., at the polarimeter level. To make this transformation, according to Eqs. (5)–(7), one will have to manipulate the three OPHELIE parameters I_H, I_V, and ϕ. In practice, because the photon energy depends mostly on I_H and I_V, we found from Eq. (2) that the only two free parameters to manipulate at first order are $\rho_{\mathrm{und}} = K_y/K_x = I_V/I_H$ and ϕ_{und}.

We started with an initial guess provided by a direct calculation of the matrix $M_{\mathrm{SU5}}(\omega)$ that involved the Fresnel constants of the various optical coatings of the beam line as described in the literature[36] and took into account of course the different incidence angles on the optics, including the 2° angle vertical elevation between mirrors M1 and M2. These calculations provided us with an initial set of ρ_{und} and ϕ_{und} values, which are listed in Table 1. We quickly found that the measured ellipses at the polarimeter level were far from pure circular polarization. We then began a cycle of trial-and-error procedures to refine these values, leading to satisfactory maximum circular polarization rates.

We used two methods to drive this procedure and minimize the number of trials, as follows:

(1) If one compares the expressions for the Stokes parameters in Eq. (4) that give the amplitudes of the electrical fields (E_{0x}, E_{0y}) associated with polarized light and those in Eqs. (5)–(7) that give the magnetic fields (K_y, K_x) that correspond to a given polarization state of the SR emitted by the OPHELIE, one can clearly see a direct analogy between the roles played by (E_{0x}, E_{0y}) and (K_y, K_x) through the relation $\rho_{\mathrm{und}} = K_y/K_x = E_{0x}/E_{0y}$ and by ($\varphi_x - \varphi_y$) and ϕ_{und}, except for the sign in Eq. (6), so one can write

$$(\varphi_x - \varphi_y)_{\mathrm{und}} = \varphi_{\mathrm{und}}{}^{\mathrm{opt}} = \pi - \phi_{\mathrm{und}}. \tag{13}$$

Therefore, starting from an initial set of $\rho_{\mathrm{und}}{}^{(1)}$ and $\phi_{\mathrm{und}}{}^{(1)}$ and leading to a measured Stokes vector $\mathbf{S}^{(1)}$, one can deduce for the next trial [indicated by a superscript (2)]

$$\rho_{\mathrm{und}}{}^{(2)} = \rho_{\mathrm{und}}{}^{(1)}\left(\frac{E_y}{E_x}\right)_{\mathrm{meas}} = \rho_{\mathrm{und}}{}^{(1)}\,\frac{1 - [S_1{}^{(1)}/S_0{}^{(1)}]}{1 + [S_1{}^{(1)}/S_0{}^{(1)}]},$$
$$\phi_{\mathrm{und}}{}^{(2)} = \phi_{\mathrm{und}}{}^{(1)}. \tag{14}$$

This measurement should cancel any remaining S_1 contribution. After a second complete measurement of the Stokes vector as described in Subsection 3.C, one may remove any remnant of S_2 by changing the phase, because a nonzero measured S_2 value means that the optical phase given by

$$\varphi_{\mathrm{meas}}{}^{\mathrm{opt}} = \cos^{-1}\left(\frac{S_2{}^{(2)}}{\{[S_0{}^{(2)}]^2 - [S_1{}^{(2)}]^2\}^{1/2}}\right) \tag{15}$$

is different from $\pm\pi/2$ (the sign depends on the helicity to be reached).

One then deduces the next trial phase:

$$\phi_{\mathrm{und}}{}^{(3)} = \phi_{\mathrm{und}}{}^{(2)} - \left(\pm\frac{\pi}{2} - \varphi_{\mathrm{meas}}{}^{\mathrm{opt}}\right). \tag{16}$$

In theory, one should perform steps (1)–(3) to get satisfactory circular polarization. In practice, because this calculation neglects the 2° elevation angle between mirrors M1 and M2, we choose to correct ρ_{und} and ϕ_{und} at the same time by injecting the Stokes

Table 1. Summary of Circular Polarization Data Measurements for RCP ($S_3 > 0$) and LCP ($S_3 < 0$) with Related Calculated ρ_{und} and ϕ_{und} Based on Published Optical Constants

Photon Energy (eV)	Harmonic Number	K_x	K_y	Expt. ρ_{und} (°)	Expt. ϕ_{und} (°)	Calc. ρ_{und} (°)[a]	Calc. ϕ_{und} (°)[b]	S_3/S_0
5.9	H1	0.88	2.41	2.74	38.0	1.86	104	0.934
6.9	H1	1.22	2.03	1.66	14.6	1.63	83	0.913
7.3	H1	1.38	1.76	1.28	3.8	1.56	75	0.903
8.0	H1	1.52	1.43	0.94	−13.5	1.44	56	0.909
8.85	H1	1.34	1.32	0.99	−68.6	1.41	42	0.961
9.6	H1	0.80	1.52	1.90	−128.5	1.36	28	0.923
10.3	H1	0.39	1.62	4.15	−127.8	1.35	17	0.927
15.2	H3	0.70	2.84	4.06	−19.9	1.37	−27	0.900[c]
16.7	H3	0.62	2.69	4.34	−15.0	1.38	−40	0.948
18.2	H3	0.62	2.50	4.03	−25.0	1.39	−48	0.911
20.0	H3	0.53	2.33	4.40	−38.0	1.38	−60	0.914
23.6	H3	0.63	2.03	3.22	−37.0	1.38	−61	0.956
27.6	H5	0.71	2.62	3.69	−39.6	1.50	−74	0.883
5.9	H1	0.80	−2.45	−3.06	32.4	2.51	110	−0.935
6.9	H1	1.22	−2.03	−1.66	14.6	1.99	85	−0.922
7.3	H1	1.38	−1.76	−1.28	3.8	1.86	66	−0.962
8.0	H1	1.52	−1.43	−0.94	−13.5	1.74	53	−0.985
8.85	H1	1.34	−1.32	−0.99	−68.6	1.63	37	−0.973
9.6	H1	0.81	−1.54	−1.90	−128.5	1.54	26	−0.995
10.3	H1	0.39	−1.62	−4.15	−127.8	1.50	16	−0.922
15.2	H3	0.58	−2.87	−4.95	−15.0	1.38	−34	−0.900[c]
16.7	H3	0.62	−2.66	−4.29	−25.0	1.37	−41	−0.969
18.2	H3	0.62	−2.50	−4.03	−25.0	1.35	−52	−0.955
20.0	H3	0.62	−2.30	−3.71	−43.0	1.34	−63	−0.980
23.6	H3	0.69	−2.00	−2.90	−39.6	1.34	−57	−0.959
27.6	H5	0.79	−2.60	−3.29	−39.6	1.45	−76	−0.922

[a]As calculated from Ref. 36 and by application of $E_x/E_y = K_y/K_x$.
[b]As calculated from Ref. 36 and by application of Eq. (13). For LCP, 180° was added to take into account the negative value of K_y.
[c]At 15.2 eV the optimized value leads to a current above the maximum current deliverable by the power supplies. This is why the S_3 value is not higher. Otherwise S_3 would be 0.99 for RCP and −0.923 for LCP. Note that, up to 20 eV, mirror M1 and the grating made from bare SiC are used, whereas above 20 eV Pt-coated versions are used instead.

parameters of vector $\mathbf{S}^{(1)}$ into Eq. (15) and iterate, in general two or three times, to get a satisfactory polarization state for which the linear parts (P_1 and P_2) are reduced to a few percent. Note that this optimization in general changes not the amount of unpolarized light (S_4/S_0) but simply the circular-to-linear polarization ratio.

(2) Another related method, somehow faster, consists of using the polarimeter first in a trivial way, i.e., inserting only one rotating element, say the second one, with azimuthal angle β. Intuitively, if the signal exhibits no modulation with β, the radiation is circularly polarized, has some unpolarized component, or both. If there is modulation, some remaining linear contribution is present. More precisely, when only one rotating element is present, Eq. (12) becomes much simpler[41]:

$$S_0 = C'\{1 - \cos(2\Psi_2)[S_1^{(1)}\cos(2\beta) + S_2^{(1)}\sin(2\beta)]\}, \quad (17)$$

where C' is a normalization constant and where $\Psi_2 = \arctan(|r_p/r_s|)$ depends on the optical constants of the polarimeter's analyzer element, which can easily be obtained by a polarization measurement in the linear polarization mode performed at the same photon energy. Therefore a simple fit of the measured flux as a function of β gives $S_1^{(1)}$ and $S_2^{(1)}$. One can then apply Eqs. (14)–(16) to refine the undulator's parameters. When the modulation in the β scan is reduced to a few percent, one can then perform the full final measurement as in Subsection 3.C, which is the only one that is able to disentangle the circular part from the nonpolarized part.

Both procedures lead to typical polarization ellipses, as shown in Fig. 7 for 10.3-eV photon energy. Here the linear contribution is reduced to ~4% for right-handed circular polarization (RCP) and to ~8% for left-handed circular polarization (LCP). This slight difference is due to the fact that we optimized the OPHELIE settings for the RCP and then simply switched the polarity of the current driving the vertical undulator. Such a polarity switch in any OPHELIE configuration would switch S_3 to $-S_3$ if there were not the 2° deflection vertical angle that is due to mirror M1, in addition to the horizontal deflection angle that couples the *s* and *p* components of the emitted SR. Therefore the optimized switch from RCP to LCP requires not only a switch in polarity of the vertical magnetic fields but also a slight change, typically in the range of a few percent (to as much as 20%), in the absolute value of the two parameters ρ_{und} and ϕ_{und} at a given photon energy. In practice, because of the limited effect on the magni-

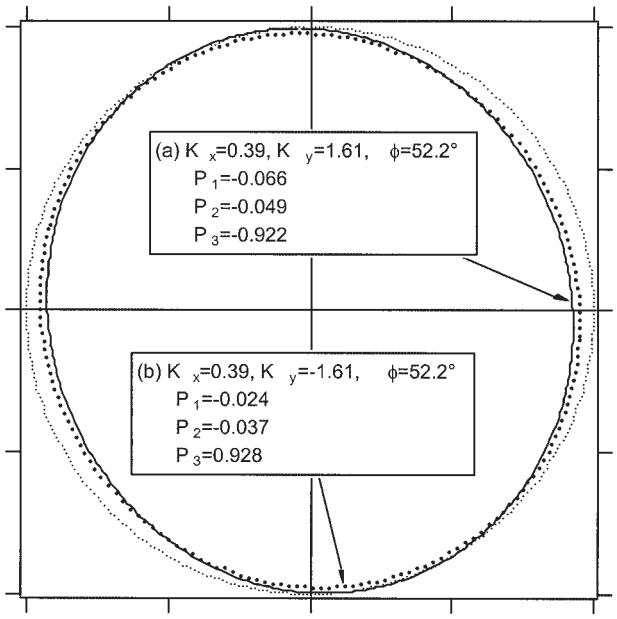

Fig. 7. Polarization ellipses recorded at 10.3 eV on the maximum of the undulator's fundamental peak for optimized circular polarization at the polarimeter level: (a) $I_H = 26.6$ A ($K_x = 0.39$), $I_V = +109.6$ A ($K_y = +1.61$), and $\phi = 52.2°$, leading to a LCP emitted SR; (b) $I_H = 26.6$ A ($K_x = 0.39$), $I_V = -109.6$ A ($K_y = -1.61$), and $\phi = 52.2°$, leading to a RCP emitted SR. The larger-dotted curve is a simple guide to the eye, showing perfect circular polarization ($S_3 = \pm 1$).

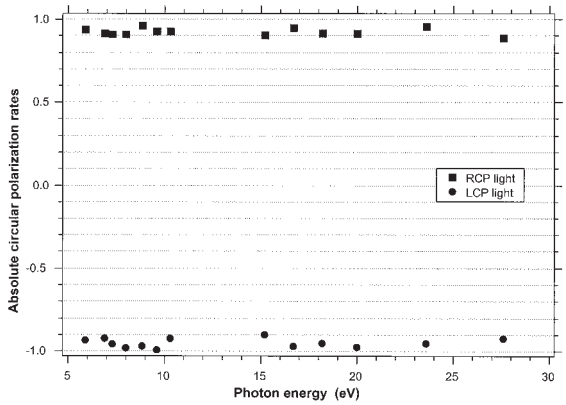

Fig. 8. Summary of all circular polarization measurements over the VUV range, showing the highest measured circular polarization rates for both RCP and LCP for the experimentally determined values of ρ_{und} and ϕ_{und} as listed in Table 1. The relative error bars are typically 2%.

tude of S_3, we would reoptimize the absolute values of ρ_{und} and ϕ_{und} if the remaining linear contribution were greater than 10% after the polarity switch.

All our circular polarization measurements over the VUV range are summarized in Fig. 8, which shows the highest measured circular polarization rates for both RCP and LCP for the experimentally determined values of ρ_{und} and ϕ_{und} as listed in Table 1. The overall performance is highly satisfactory, with a minimum circular polarization rate of 88% but a typical rate of 92–95% or better. Because the linear part has been reduced to a few percent, from Eq. (8) one can write that

$$\frac{S_4}{S_0} \approx 1 - \frac{|S_3|}{S_0} = 1 - P_c. \tag{18}$$

The set of data as shown in Fig. 8 that spans the whole VUV range is to our knowledge unique and allows one to perform any CD experiment easily, in terms of both the circular polarization rate values by themselves and of accurate knowledge of these values. Note that because of the weak transmitted flux through the polarimeter, which is probably due to the relatively low K value of the vertical undulator that has not been compensated for in terms of flux by an important K value of the horizontal undulator, it has not been possible to determine ρ_{und} and ϕ_{und} at 10.3–15.2 eV by use of the full procedure described above. Nevertheless, if necessary, one could use approach method (2) to determine these parameters by making simple β scans but of course with no possibility of disentangling the circular from the nonpolarized part.

As can be deduced from Table 1, the mean RCP rate is 92.1 ± 2.3%, and the mean LCP rate is 95.2 ± 2.9%. The slight discrepancy between RCP and LCP values, which leads to a higher nonpolarized contribution for RCP (~8%) than of LCP (~4%), is probably due to an imperfect trajectory inside the vertical undulator whose polarity is being switched. This is confirmed when one compares the experimentally determined and calculated ρ_{und} values. Indeed, except near 8–9 eV the experimental ρ_{und} values are much higher than the calculated values, although the overall trend is somehow reproduced on the low-energy part. This can be so because of a mismatch of the published optical constants[36] and the effective values that are applicable to our optics in their real environment (including their evolution with pollution). There may also be a certain weakness in the efficiency of the vertical undulator that is due, for instance, to an S-shaped or off-center trajectory inside the insertion device, probably because of some imperfect K-dependent settings of correcting coils or because of the presence of some inhomogeneous magnetic fields. This effect seems to dominate the emittance effect, which, at the Super-ACO storage ring, would affect vertical and horizontal linear polarization in the same way. Such an undulator defect would be consistent with the observation that the measured circular polarization rates are lower on the fifth harmonic than on the third harmonic, presumably because the SR emissions do not perfectly interfere at each wiggle of the undulator.

Note that this is to our knowledge the first time that a polarization analysis has been performed of the harmonics of an Onuki-type crossed undulator, because previously published data concern only the fundamental radiation.[15,43] Of course our analysis is possible because of the specific geometry of the beam line, which is such that, to get a circular polarization on the sample, one starts from elliptical po-

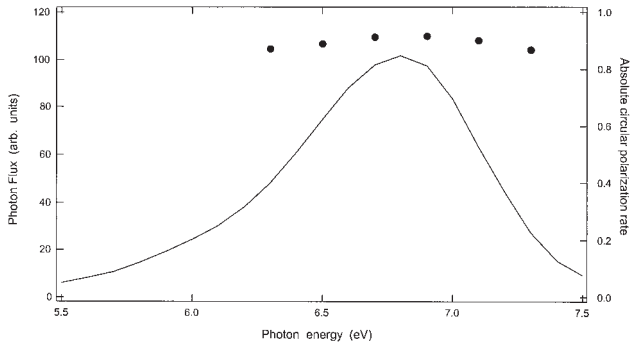

Fig. 9. Undulator spectrum (left-hand scale) for RCP near 6.9 eV with $\rho_{und} = -1.66$ and $\phi_{und} = 14.6°$, together with the measured absolute values of P_c at several photon energies (right-hand scale).

larization quite far from circular polarization. Therefore there is no need here to compromise between circular polarization rates and flux on the harmonics, as it is with pure grazing-incidence beam lines operating in the soft-x-ray range.[44]

Between the measured photon energies listed in Table 1 it is of course possible to interpolate the measured ρ_{und} and ϕ_{und}, but it is also possible to set the monochromator on the blue or the red side of the maximum of the undulator spectrum. Moreover, some aspects of the SU5 scientific case deal with the irradiation of amino acids with the undispersed white beam of the undulator, with the monochromator used at zeroth order.[25] As the sample will integrate the whole undulator spectrum, it is necessary to measure the variation of the circular polarization rates over the undulator spectrum for fixed ρ_{und} and ϕ_{und} settings. Such a measurement, at ~6.9 eV, is presented in Fig. 9 for RCP. Starting from a maximum value of 91.3% at the peak of the spectrum, the circular polarization rate P_c gently decreases, in quite a symmetric way on both sides, to 87% on the side at 0.5 eV from the maximum, a satisfactory level that allows one to use the full undulator spectrum centered at 6.9 eV. Note that this slight reduction of P_c is due mostly to the rapid variations of the optical constants in this energy range (see Table 1) rather than to an intrinsic depolarization effect in the undulator's emission.

Finally, we checked the effect on the circular polarization rates of the commonly used low-energy-pass filters, such as LiF and MgF_2 windows and the SU5 absorption gas cell filter,[37] that are used to suppress the harmonics of the undulator that could be transmitted by the high orders of diffraction of the gratings. None of these filters produces any measurable effect on the polarization: not the LiF plate, because it is perfectly amorphous and isotropic, not the MgF_2 window, because although it is a birefringent material we use only windows cut in such a way that the optical main axis corresponds to the photon propagation axis, and not the gas filter because, in its working pressure range (as much as ~1 Torr), one can neglect the light scattering by the rare-gas atoms that fill the filter.

5. Conclusion

We have presented a comprehensive polarization study of the whole SU5 beam line in both linear and the circular polarization modes, showing the versatility of the undulator OPHELIE and the great utility of its dedicated polarimeter, which allows us to cope with the polarization modifications induced by different optics. The SU5 beam line is therefore fully calibrated in terms of polarization capabilities, with satisfactory circular polarization rates. To our knowledge, these are the highest rates reported in the VUV range. Despite some uneven efficiency with the photon energy, the OPHELIE crossed undulator behaves as expected in terms of polarization, permitting complete control of the emitted polarization by manipulation of ρ_{und} and ϕ_{und} for a given photon energy both in the fundamental peak and in the harmonics.

The whole beam line, including the polarimeter, is expected to be transferred to the next French synchrotron ring, SOLEIL, with a new 10-m-long variable-polarization undulator that should provide increased flux associated with a faster polarization switching speed, allowing LD and CD experiments to be performed at a targeted frequency of 1 Hz.

We warmly thank the technical staff of the LURE, especially the Machine Department staff, which has been strongly involved in the commissioning of the OPHELIE and made possible its transparent operation for all the users, as well as J. L. Marlats and D. Nether for their outstanding mechanical design of the polarimeter, D. Lefebvre, E. Labrude, and S. Denise for the careful mounting of the polarimeter, B. Pilette and J. M. Berset for their help in the vacuum conception of the polarimeter and its commissioning, M. Marie and A. Petit for their contribution to writing the acquisition software, and B. Lagarde and F. Polack for their help in the choice of the optics and their alignment.

References

1. U. Heinzmann and N. A. Cherepkov, "Spin polarization in photoionization," in *VUV and Soft X-Ray Photoionization*, U. Becker and D. Shirley, eds. (Plenum, New York, 1996), pp. 521–559.
2. G. Schönhense and J. Hormes, "Photoionization of oriented systems and circular dichroism," in *VUV and Soft X-Ray Photoionization*, U. Becker and D. Shirley, eds. (Plenum, New York, 1996), pp. 607–652.
3. F. Schäfers, W. Peatman, A. Eyers, Ch. Heckenkamp, G. Schönhense, and U. Heinzmann, "High-flux normal incidence monochromator for circularly polarized synchrotron radiation," Rev. Sci. Instrum. **57,** 1032–1041 (1986).
4. W. B. Westerveld, K. Becker, P. W. Zetner, J. J. Corr, and J. W. McConkey, "Production and measurement of circular polarization in the VUV," Appl. Opt. **24,** 2256–2262 (1985).
5. H. Höchst, R. Patel, and F. Middleton, "Multiple-reflection $\lambda/4$ phase shifter: a viable alternative to generate circular-polarized synchrotron radiation," Nucl. Instrum. Methods A **347,** 107–114 (1994).
6. P. A. Snyder, "Status of natural and magnetic circular dichroism instrumentation using synchrotron radiation," Nucl. Instrum. Methods A **222,** 364–371 (1984).

7. P. Elleaume, "Generation of various polarization states from insertion devices: a review," Rev. Sci. Instrum. **60,** 1830–1833 (1989).
8. R. P. Walker and B. Diviacco, "Studies of insertion devices for producing circularly polarized radiation with variable helicity in ELLETRA," Rev. Sci. Instrum. **63,** 332–335 (1992).
9. J. Bahrdt, W. Fentrup, A. Gaupp, M. Scheer, W. Gudat, G. Ingold, and S. Sasaki, "Ellipically polarizing insertion devices at BESSY II," Nucl. Instrum. Methods A **467-468,** 21–29 (2001), and references therein.
10. L. Museur, C. Olivero, D. Riedel, and M. C. Castex, "Polarization properties of coherent VUV light at 125 nm generated by sum-frequency four-wave mixing in mercury," Appl. Phys. B **70,** 1–5 (2000).
11. P. Antoine, A. L'Huillier, M. Lewenstein, P. Salières, and B. Carré, "Theory of high-order harmonic generation by an elliptically polarized laser field," Phys. Rev. A **53,** 1725–1745 (1996).
12. S. Motoki, J. Adachi, K. Ito, K. Ishii, K. Soejima, A. Yagishita, S. K. Semenov, and N. A. Cherepkov, "Direct probe of the shape resonance mechanism in $2\sigma_g$-shell photoionization of the N_2 molecule," Phys. Rev. Lett. **88,** 063003 (2002).
13. D. Desiderio, S. DiFonzo, B. Diviacco, W. Jark, J. Krempasky, R. Krempaska, F. Lama, M. Luce, H. C. Mertins, M. Piacentini, T. Prosperi, S. Rinaldi, G. Soullie, F. Schäfers, S. Turcini, R. P. Walker, and N. Zema, "The ELETTRA circular polarization beamline and electromagnetic elliptical wiggler insertion device," Synchr. Rad. News **12,** 34–38 (1999).
14. G. Rybalchenko, K. Shirasawa, M. Morita, N. Smolyakov, K. Goto, T. Matsui, and H. Hiraya, "Performance and future plan of multimode undulator at HiSOR," Nucl. Instrum. and Methods A **467-468,** 173–176 (2001).
15. M. Yuri, K. Yagi, T. Yamada, and H. Onuki, "Polarization characteristics of polarizing undulator radiation installed in the electron storage ring NIJI-II," J. Electron Spectrosc. Relat. Phenom. **80,** 501–504 (1996).
16. T. Koide, T. Shidara, M. Yuri, N. Kandaka, K. Yamaguchi, and H. Fukutani, "Elliptical-polarization analyses of synchrotron radiation in the 5–80 eV region with a reflection polarimeter," Nucl. Instrum. Methods A **308,** 635–644 (1991).
17. T. Koide, T. Shidara, and M. Yuri, "Polarization analyses of elliptically polarized vacuum-ultraviolet undulator radiation," Nucl. Instrum. Methods A **336,** 368–372 (1993).
18. F. Schäfers, H.-C. Mertins, A. Gaupp, W. Gudat, M. Mertin, I. Packe, F. Schmolla, S. Di Fonzo, G. Souillie, W. Jark, R. Walker, X. Le Cann, R. Nyholm, and M. Eriksson, "Soft-x-ray polarimeter with multilayer optics: complete analysis of the polarization state of light," Appl. Opt. **38,** 4074–4088 (1999).
19. L. Nahon, M. Corlier, P. Peaupardin, F. Marteau, O. Marcouillé, P. Brunelle, C. Alcaraz, and P. Thiry, "A versatile electromagnetic planar/helical crossed undulator optimized for the SU5 low energy/high resolution beamline at Super-ACO," Nucl. Instrum. Methods A **396,** 237–250 (1997).
20. L. Nahon, B. Lagarde, F. Polack, C. Alcaraz, O. Dutuit, M. Vervloet, and K. Ito, "A new VUV high-resolution undulator-based beamline at Super-ACO," Nucl. Instrum. Methods A **404,** 418–429 (1998).
21. L. Nahon, C. Alcaraz, J.-L. Marlats, B. Lagarde, F. Polack, R. Thissen, D. Lepère, and K. Ito, "Very-high spectral resolution obtained with SU5: a VUV undulator-based beamline at Super-ACO," Rev. Sci. Instrum. **72,** 1320–1329 (2001).
22. M. Meyer, S. Aloïse, P. O'Keefe, and A. N. Grum-Grzhimailo, "Polarization effects in the photoionization of VUV excited atoms," in *Correlation, Polarization and Ionization of Atomic Systems*, G. F. Hanne, ed., AIP Conf. Proc. **697,** 42–47 (2003).
23. M. Lebech, J. C. Houver, A. Lafosse, D. Dowek, C. Alcaraz, L. Nahon, and R. Lucchese, "Complete description of linear molecule photoionization achieved by vector correlations using light of a single circular polarization," J. Chem. Phys. **118,** 9653–9663 (2003).
24. G. Garcia, L. Nahon, M. Lebech, J.-C. Houver, D. Dowek, and I. Powis, "Circular dichroism in the photoelectron angular distribution from randomly oriented enantiomers of camphor," J. Chem. Phys. **119,** 8781–8784 (2003).
25. U. Meierhenrich, B. Barbier, R. Jacquet, A. Chabin, C. Alcaraz, L. Nahon, and A. Brack, "Photochemical origin of biomolecular asymmetry," Astrobiology **2,** 167–170 (2001).
26. C. Alcaraz, R. Thissen, M. Compin, A. Jolly, M. Drecher, and L. Nahon, "First polarization measurements of OPHELIE: a versatile polarization VUV undulator at Super-ACO," in *X-Ray Optics: Design, Performance, and Applications*, A. Khounsary, A. Freund, T. Ishikawa, G. Srajer, and J. Lang, eds., Proc. SPIE **3773,** 250–261 (1999).
27. H. Onuki, "Elliptically polarized synchrotron radiation source with crossed and retarded magnetic fields," Nucl. Instrum. Methods A **246,** 94–98 (1986).
28. H. Onuki, N. Saito, and T. Saito, "Undulator generating any kind of elliptically polarized radiation," Appl. Phys. Lett. **52,** 173–175 (1988).
29. M. Corlier, P. Brunelle, C. Herbeaux, O. Marcouillé, J. L. Marlats, F. Marteau, P. Peaupardin, M. Sommer, J. Vétéran, and L. Nahon, "A planar/helicoidal electromagnetic crossed overlapped undulator at LURE," in *Proceedings of the 15th International Conference on Magnet Technology*, L. Liangzhen, S. Gualiao, and S. Luguang, eds. (Science Press, Beijing, 1998), pp. 84–87.
30. M. Corlier, J.-C. Besson, P. Brunelle, J. Claverie, J.-M. Godefroy, C. Herbeaux, D. Lefebvre, O. Marcouillé, J.-L. Marlats, F. Marteau, J. Michaut, P. Peaupardin, A. Petit, M. Sommer, J. Vétéran, and L. Nahon, "Commissioning of OPHELIE: the new electromagnetic crossed overlapped undulator at Super-ACO," in *Proceedings of PAC '99*, A. Luccio and W. Mackay, eds. (Institute of Electrical and Electronics Engineers, Piscataway, N.J., 2000), pp. 2686–2688.
31. L. Nahon, P. Peaupardin, F. Marteau, O. Marcouillé, P. Brunelle, R. Thissen, C. Alcaraz, and M. Corlier, "Commissioning of OPHELIE in the DC mode: an electromagnetic planar/helical crossed VUV undulator at Super-ACO," Nucl. Instrum. Methods Phys. Res. A **447,** 569–586 (2000).
32. R. T. Holm, "Convention confusions," in *Handbook of Optical Constants of Solids*, 2nd ed., E. D. Palick, ed. (Academic, New York, 1991), pp. 21–55.
33. P. Elleaume, "Helios: a new type of linear/helical undulator," J. Synchr. Rad. **1,** 19–26 (1994).
34. P. Brunelle, J.-C. Besson, L. Cassinari, J. Claverie, J. Darpentigny, M. Corlier, J.-M. Godefroy, O. Marcouillé, F. Marteau, A. Nadji, A. Petit, M. Sommer, and L. Nahon, "Transparent user operation of OPHELIE at Super-ACO," in *Proceedings of EPAC 2000*, J.-L. Laclare, W. Mitaroff, Ch. Petit-Jean-Genaz, J. Poole, and M. Regler, eds. (Austrian Academy of Sciences Press, Vienna, 2000), pp. 1013–1015.
35. For a general introduction to the various polarization formalisms see D. Kliger, J. Lewis, and C. Randall, *Polarized Light in Optics and Spectroscopy* (Academic, San Diego, Calif., 1990).
36. E. D. Palick, *Handbook of Optical Constants of Solids*, 2nd ed. (Academic, San Diego, Calif., 1991).
37. B. Mercier, M. Compin, C. Prevost, G. Bellec, R. Thissen, O. Dutuit, and L. Nahon, "Experimental and theoretical study of a differentially-pumped absorption gas cell used as a low energy-pass filter in the VUV photon energy range," J. Vac. Sci. Technol. A **18,** 2533–2541 (2000).
38. K. J. Kim, "Characteristics of synchrotron radiation," in *Proceedings of the AIP Conference on the Physics of Particle Accelerators*, AIP Conf. Proc. **184,** 565–632 (1989).
39. Alessandro Mirone, Optics Group, LURE, Orsay, France (personal communication, 1999).

40. K. Rabinovitch, L. R. Canfield, and R. P. Madden, "A method for measuring polarization in the vacuum ultraviolet," Appl. Opt. **4,** 1005–1010 (1965).
41. C. Alcaraz, D. Nether, J.-L. Marlats, B. Pilette, and L. Nahon, are preparing a paper to be called "Conception and performances of a very-accurate reflection polarimeter optimized for the VUV range."
42. T. Koide, T. Shidara, M. Yuri, N. Kandaka, and H. Fukutani, "Production and direct measurement of circularly polarized vacuum-ultraviolet light with multireflection optics," Appl. Phys. Lett. **58,** 2592–2594 (1991).
43. K. Yagi, H. Onuki, S. Sugiyama, and T. Yamazaki, "Absolute spectral brightness and polarization characteristics of radiation from a polarizing undulator in the visible region," Rev. Sci. Instrum. **63,** 396–399 (1992).
44. See, for instance, P. Elleaume and J. Chavanne, "A new powerful flexible linear/helical undulator for soft x-rays," Nucl. Instrum. Methods A **304,** 719–724 (1991).